Journal of Pharmaceutical Analysis 12 (2022) 824–838

Contents lists available at ScienceDirect

Journal of Pharmaceutical Analysis

journal homepage: www.elsevier.com/locate/jpa

Original article

Rabdosia serra alleviates dextran sulfate sodium salt-induced colitis in mice through anti-inflammation, regulating Th17/Treg balance, maintaining intestinal barrier integrity, and modulating gut microbiota

Hongyi Li [a, 1], Yi Wang [b, 1], Shumin Shao [a], Hui Yu [c], Deqin Wang [c], Chuyuan Li [c], Qin Yuan [a], Wen Liu [a], Jiliang Cao [d], Xiaojuan Wang [e], Haibiao Guo [c], Xu Wu [b, *], Shengpeng Wang [a, f, **]

[a] State Key Laboratory of Quality Research in Chinese Medicine, Institute of Chinese Medical Sciences, University of Macau, Macao, 999078, China
[b] Laboratory of Molecular Pharmacology, Department of Pharmacology, School of Pharmacy, Southwest Medical University, Luzhou, Sichuan, 646000, China
[c] Hutchison Whampoa Guangzhou Baiyunshan Chinese Medicine Co., Ltd., Guangzhou, 510000, China
[d] College of Pharmacy, Shenzhen Technology University, Shenzhen, Guangdong, 518118, China
[e] School of Pharmacy, Lanzhou University, Lanzhou, 730000, China
[f] Macau Centre for Research and Development in Chinese Medicine, University of Macau, Macao, 999078, China

ARTICLE INFO

Article history:
Received 22 December 2021
Received in revised form
27 July 2022
Accepted 2 August 2022
Available online 18 August 2022

Keywords:
Rabdosia serra
Chemical profile
Colitis
Inflammation
Gut microbiota

ABSTRACT

Rabdosia serra (*R. serra*), an important component of Chinese herbal tea, has traditionally been used to treat hepatitis, jaundice, cholecystitis, and colitis. However, the chemical composition of *R. serra* and its effect against colitis remain unclear. In this study, the chemical composition of the water extract of *R. serra* was analyzed using ultra performance liquid chromatography coupled with a hybrid linear ion trap quadrupole-orbitrap mass spectrometer (UPLC-LTQ-Orbitrap-MS). A total of 46 compounds, comprising *ent*-kaurane diterpenoids, flavonoids, phenolic acids, and steroids, were identified in the water extract of *R. serra*, and the extract could significantly alleviate dextran sulfate sodium salt-induced colitis by improving colon length, upregulating anti-inflammatory factors, downregulating proinflammatory factors, and restoring the balance of T helper 17/T regulatory cells. *R. serra* also preserved intestinal barrier function by increasing the level of tight junction proteins (zonula occludens 1 and occludin) in mouse colonic tissue. In addition, *R. serra* modulated the gut microbiota composition by increasing bacterial richness and diversity, increasing the abundance of beneficial bacteria (*Muribaculaceae*, *Bacteroides*, *Lactobacillus*, and *Prevotellaceae_UCG-001*), and decreasing the abundance of pathogenic bacteria (*Turicibacter*, *Eubacterium_fissicatena_group*, and *Eubacterium_xylanophilum_group*). Gut microbiota depletion by antibiotics further confirmed that *R. serra* alleviated colitis in a microbiota-dependent manner. Overall, our findings provide chemical and biological evidence for the potential application of *R. serra* in the management of colitis.

1. Introduction

Inflammatory bowel disease (IBD), which mainly includes Crohn's disease (CD) and ulcerative colitis (UC), is a chronic and multifactorial inflammatory disease of the intestinal tract [1]. Over the last few decades, the incidence of IBD increased by more than two times in several East Asian countries and will continue to increase in next decade [2]. Recent studies have indicated that IBD is closely related to disrupted intestinal barrier function and immune function imbalance [3–5]. Moreover, changes in the diversity, structural composition, and function of the intestinal microbiome caused by abnormal inflammatory response can lead to the development of IBD [6–8]. The intestinal microbiome plays a critical role in nutrition uptake, immune response, metabolism, and pathogen defense [9].

Peer review under responsibility of Xi'an Jiaotong University.
* Corresponding author.
** Corresponding author. State Key Laboratory of Quality Research in Chinese Medicine, Institute of Chinese Medical Sciences, University of Macau, Macao, 999078, China.
E-mail addresses: wuxulz@126.com (X. Wu), swang@um.edu.mo (S. Wang).
[1] Both authors contributed equally to this work.

https://doi.org/10.1016/j.jpha.2022.08.001

Current treatments for IBD include aminosalicylates (e.g., 5-aminosalicylic acid (5-ASA) and mesalazine), corticosteroids (e.g., methylprednisolone and dexamethasone), antibiotics (e.g., metronidazole and ciprofloxacin), immunomodulators (e.g., methotrexate and 6-mercaptopurine), biological agents, and surgery in severe IBD cases [10,11]. However, owing to the limited therapeutic efficacy, high economic cost, and side effects of long-term treatments, there is an urgent need to discover novel effective drugs for IBD treatment. Previous studies have reported phytotherapy as one of the most valuable therapies for the management of intestinal disorders [7,12]. Certain medicinal herbs, such as *Abelmoschus Manihot* [7], *Rhodiola crenulate* [12], *Curcuma longa* [13], and *Ginkgo biloba* [14], and their derived natural compounds have received considerable attention for their marked alleviation of IBD symptoms.

Rabdosia serra (*R. serra*) (Maxim.) Hara (genus of *Isodon*), also known as "Xihuangcao", is mainly distributed in the southern regions of China, including Guangdong, Fujian, and Guangxi, as well as other subtropical and tropical parts of Asia [15–17]. It is one of the most important herbs in Chinese herbal tea. In China, it has long been used as a local indigenous medicine for the treatment of enteritis, jaundice, hepatitis, and acute cholecystitis [17]. Although the chemical profile of *R. serra* is unclear, previous phytochemical studies have shown that *ent*-kaurane diterpenoids, flavonoids, phenolic acid, and steroids are its main bioactive constituents [18–20]. Some of these compounds exhibit promising antioxidative, antiinflammatory, antihypotonic, antibacterial, and anticancer activities [16,19,21–23]. Furthermore, oridonin and its derivatives from plants belonging to the genus *Isodon* have been shown to inhibit the proliferation of splenic Th1/Th17 cells and affect memory $CD4^+$ T cells in trinitrobenzene sulfonic acid-induced colitis. Because of their abundant diterpenes, *Isodon* plants have recently been shown to have a significant effect on colorectal cancer treatment [22,23]. Furthermore, the dietary supplementation of oridonin, the main *ent*-kaurane diterpenoid in *Isodon* plants, can significantly improve intestinal health [24]. Therefore, investigating the effects of *R. serra* against IBD and the underlying mechanisms is clinically relevant.

This study aimed to investigate the effects of the water extract of *R. serra* as a dietary supplement on dextran sulfate sodium (DSS) salt-induced colitis as well as its interaction with the gut microbiota, inflammatory factors, tight junction proteins, and T helper 17 (Th17)/regulatory T (Treg) cells and its regulation of the gut microbiota. In addition, the chemical components of the water extract of *R. serra* were analyzed using ultra-performance liquid chromatography coupled with linear trap quadrupole-Orbitrap mass spectrometry (UPLC-LTQ-Orbitrap-MS).

2. Materials and methods

2.1. Chemicals and materials

Reference standards, including caffeic acid, quercetin, isoquercitrin, ferulic acid, vitexin, vicenin II, schaftoside, isoschaftoside, rutin, hyperoside, salicylic acid, rosmarinic acid, daidzein, oleanolic acid, stigmasterol, epinodosin, methyl rosmarinate, kamebakaurin, shikokianin, lasiokaurin, oridonin, lasiodonin, ponicidin, and nodosin were purchased from Refmedic Biotechnology Co., Ltd. (Chengdu, China). Additionally, 5-ASA was purchased from Aladdin Biochemical Technology Co., Ltd. (Shanghai, China), while DSS (molecular weight: 36–50 kDa) was obtained from International Laboratory USA (San Francisco, CA, USA). The antibiotics, namely, vancomycin, neomycin sulfate, ampicillin, and metronidazole, were purchased from Shanghai Macklin Biochemical Co., Ltd. (Shanghai, China). Mouse serum interleukin (IL)-17, IL-4, transforming growth factor (TGF)-β1, and interferon (IFN)-γ enzyme-linked immunosorbent assay (ELISA) kits were obtained from Novus Biologicals (Littleton, CO, USA). A lipopolysaccharide (LPS) ELISA kit was provided by CUSABIO (Wuhan, China). A fixation/permeabilization solution kit (BD GolgiPlug) and CD25, Foxp3, CD4, and IL-17A antibodies used for Th17 and Treg cell phenotyping were purchased from BD Biosciences (Franklin Lakes, NJ, USA).

2.2. Preparation of the water extract of R. serra

The aerial parts of air-dried *R. serra* (100 g) were boiled (100 °C) in ultrapure water (600 mL) for 1 h. This step was repeated twice under the same extraction conditions; then both the samples were centrifuged (5,000 rpm for 10 min at 4 °C) and the supernatants were pooled. This supernatant was concentrated and dried in vacuo to yield a 10.3 g of the water extract of *R. serra*.

2.3. UPLC-LTQ-Orbitrap-MS for chemical characterization

The chemical analysis of the water extract of *R. serra* was performed based on our previously reported methods with slight modification [25,26]. UPLC-LTQ-Orbitrap-MS analysis was performed using a DionexUltiMate 3000 rapid separation binary UPLC system (Thermo Fisher Scientific Inc., Bremen, Germany) equipped with an LTQ-Orbitrap XL mass spectrometer and electrospray ionization (ESI) source. Hypersil gold C_{18} column (150 mm × 2.1 mm, 1.9 μm) was used for the chromatographic separation at 35 °C. Formic acid (0.1%, *V/V*) solution (A) and acetonitrile (B) were used as mobile phases. The gradient elution program was performed as follows: 0–2 min, 5% B; 2–25 min, 5%–95% B; 25–28 min, 95% B; 28–29 min, 95%–5% B; 29–30 min, 5% B. The flow rate was set at 0.4 mL/min, and 4 μL of the water extract of *R. serra* (final concentration of 0.5 mg/mL) was injected for analysis.

Detection using LTQ-Orbitrap-MS was performed in both negative and positive ESI modes. The MS parameters of the positive/negative ion modes were as follows: capillary temperature, 380 °C/380 °C; capillary voltage, +35 V/−35 V; ion spray voltage, +4.5 kV/−4.5 kV; and tube lens voltage, +110 V/−100 V. Reference masses were recorded at an *m/z* range of 100–1,500.

2.4. Animal experiments

All animal experiments and animal care procedures were performed in accordance with the guidelines of Committee on Use and Care of Animals of Southwest Medical University (reference no.: 2020226). SPF-grade C57BL/6 male mice aged 6–8 weeks were obtained from Spelford Biotechnology Co., Ltd. (Beijing, China) and housed under pathogen-free conditions in a regular 12 h light/dark cycle at 22 °C ± 2 °C and relative humidity of 55%–60%. The mice were given *ad libitum* access to food and sterilized water. All mice were acclimatized for 7 days before the experiment.

Mice were randomly divided into five groups ($n = 8$) as follows: control, DSS, 5-ASA (positive control), *R. serra* (RS)-75, and RS-150. Mice in the DSS, 5-ASA, RS-75, and RS-150 groups were administered with DSS (2.8%, *m/V*) in sterilized drinking water for 6 days (from day 0 to day 6) to induce acute colitis. From day 5 to day 10, mice in the DSS, 5-ASA, RS-75, and RS-150 groups were orally administered with water, 5-ASA (100 mg/kg), *R. serra* (75 mg/kg), and *R. serra* (150 mg/kg), respectively, daily. The control group was orally administered with water daily. Body weight change and disease activity index (DAI) score were assessed daily. The DAI score criteria are outlined in Table S1. On days 0 and 10, mouse feces were collected and stored at −80 °C within 2 h for further microbial analysis. On day 11, mice were euthanatized and their entire colons were excised. The colons were measured and then washed gently

with phosphate-buffered saline (PBS, pH = 7.4). Blood was collected and centrifuged to obtain serum samples for ELISA.

2.5. Histological analysis

Hematoxylin and eosin (H&E) staining of colonic tissue was performed for histological analysis as previously described [12]. Briefly, distal colon segments (approximately 1 cm) were fixed in formalin (4%, *m*/*V*) and embedded in paraffin after dehydration. Subsequently, images of the H&E stained sections were acquired using a Nikon Eclipse Ts2R + FL microscope (Nikon Instruments Inc., Tokyo, Japan). The histological score was recorded according to the previously reported criteria [12].

2.6. Evaluation of inflammatory factors

The serum and colonic levels of pro-inflammatory (IL-17 and IFN-γ) and anti-inflammatory (TGF-β1 and IL-4) factors were evaluated using ELISA kits according to the manufacturer's instructions.

2.7. Flow cytometry analysis

Mouse mesenteric lymph nodes (MLNs) were harvested and gently pressed through a cell strainer in precooled PBS to obtain a single cell suspension (1×10^6 cells/mL). For Th17 cell intracellular staining, single cells were prestimulated using GolgiPlug (purchased from BD Biosciences, Franklin Lakes, NJ, USA) for 6 h at 37 °C at a concentration of 1 μL/mL. For the staining of cell surface markers, cells were incubated with anti-CD4 antibody at 4 °C for 30 min in the dark and then fixated and permeabilized for 20 min under the same conditions. Subsequently, the cells were incubated with anti-IL-17A antibody for 1 h at 4 °C for intracellular staining. For the staining of Treg cells, single cells were incubated with anti-CD25 antibody for 0.5 h. After fixation and permeabilization, the cells were stained with anti-Foxp3 antibody at 4 °C for 1 h in the dark. The flow cytometric experiment was performed using FACSVerse (BD Biosciences), and the data were analyzed using FlowJo 10 software (TreeStar, San Carlos, CA, USA).

2.8. Immunohistochemical (IHC) analysis

To determine the colonic levels of tight junction proteins (such as zonula occludens 1 (ZO-1) and occludin), IHC analysis was performed according to our previously reported method [12]. Briefly, after deparaffinization, rehydration, and antigen retrieval, the colonic sections were treated with H_2O_2 (3%, *V*/*V*) to block endogenous peroxidase and then incubated with bovine serum albumin (3%, *m*/*V*). Colonic sections were then incubated with primary antibodies against ZO-1 and occludin at 4 °C overnight in the dark. After washing with PBS, the slides were immersed in corresponding horseradish peroxidase-linked secondary antibodies. Antibody signals were visualized with diaminobenzidine (DAB) and hematoxylin under an optical microscope. Positive DAB-stained areas were quantified using the ImageJ software (Version 1.48v, National Institute of Health, Bethesda, MD, USA).

2.9. 16S rRNA analysis

Microbiome DNA extraction and 16S rRNA gene sequencing were performed according to our previously reported method [12]. 16S rRNA gene sequencing was performed on an Illumina MiSeq platform according to the manufacturer's instruction (Majorbio Bio-Pharm Technology Co., Ltd., Shanghai, China).

The diversity of the gut microbiota was analyzed using Majorbio Cloud Platform. 16S rRNA raw fastq files were demultiplexed and quality-filtered using Trimmomatic [12]. Operational taxonomic units (OTUs) were clustered with 97% sequence similarity using UPARSE. UCHIME and Silva (SSU123) were used for chimeric sequences and taxonomy, respectively. R tools accompanied with the package mixOmics were used for principal coordinate analysis (PCoA) and partial least squares discriminant (PLS-DA) analysis. Distance-based redundancy analysis (db-RDA) and Spearman correlation were performed to analyze the correlation of microbial structure change with colitis abnormalities.

2.10. Statistical analysis

Statistical analysis was performed using the GraphPad Prism 8.0 software (GraphPad Software, La Jolla, CA, USA), and the results are expressed as means ± standard deviation. One-way analysis of variance followed by a post hoc Tukey's test was used for multiple group comparisons. *P* value less than 0.05 was considered statistically significant.

3. Results and discussion

3.1. Chemical analysis of the water extract of R. serra

Previous studies reported that *R. serra* extracts contain diterpenoids, triterpenoids, flavonoids, phenolic acids, and other chemical compounds [15,16,19,27–29]. As shown in Fig. 1 and Table S2, a total of 46 compounds, including *ent*-kaurane diterpenoids, flavonoids, phenolic acid, steroids, and other compounds, were rapidly identified in the water extract of *R. serra* through UPLC-LTQ-Orbitrap-MS analysis by comparison with reference standards and/or a previous report [18]. The representative chromatograms are shown in Figs. 1A and B.

As shown in Fig. 1C, a total of 19 *ent*-kaurane diterpenoids, including 3 C-20-nonoxygenated *ent*-kaurane diterpenoids and 16 C-20-oxygenated *ent*-kaurane diterpenoids (nine 7,20-*epoxy*-*ent*-kaurane, four enmein type, one 7,20-diepoxy-*ent*-kaurane, one 3,20-*epoxy*-*ent*-kaurane, and one spiro-lactone type) were tentatively identified. The C-20-nonoxygenated type, including compounds **26** (amethystonoic acid), **34** (umbrosin B), and **44** (inflexarabdonin J), were tentatively identified in the extract. The continuous loss of neutral H_2O (−18 Da) at C-7 and C-11 was observed through cleavage of a hydroxyl group. Taking amethystonoic acid as an example, the *m*/*z* values 345 ($[M-H-H_2O]^-$) and 327 ($[M-H-2H_2O]^-$) were obtained through a successive loss of H_2O. Moreover, the characteristic ion fragments at *m*/*z* 301 ($[M-H-H_2O-CO_2]^-$) and *m*/*z* 283 ($[M-H-2H_2O-CO_2]^-$) were obtained through the cleavage of the hydroxyl group at C-7 and loss of CO_2 of the carbonyl group at C-15.

The 7,20-*epoxy*-*ent*-kaurane diterpenoids included compounds **7** (1-*α*-*O*-*β*-D-glucopyranosyl enmenol), **13** (shikokiaside A), **16** (rubescensin S), **23** (rabdosinate), **25** (lasiokaurin), **27** (lasiokaurinol), **28** (megathyrin A), **37** (effusanin A), and **38** (rabdocoetsin). Compound **28**, a representative 7,20-*epoxy*-*ent*-kaurane diterpenoid, was characterized by its loss of 18 Da ($-H_2O$) successively from a hydroxyl group at C-1 and C-14 to give a fragment at *m*/*z* 329 ($[M-H-H_2O]^-$) and 311 ($[M-H-2H_2O]^-$). Simultaneously, the distinctive fragment ions at *m*/*z* 301 and 271 were identified by their loss of CO ($[M-H-H_2O-28\ Da]^-$) from the D ring and CH_2O ($[M-H-H_2O-CO-30\ Da]^-$) from the C-20 oxygenated B ring. Similar cleavage patterns were observed in the other 7,20-*epoxy*-*ent*-kaurane diterpenoids.

Maoecrystal A was the only 3,20-*epoxy*-*ent*-kaurane diterpenoid found in the water extract of *R. serra*. In an ESI positive mode, it exhibited an ion peak $[M-H]^+$ at *m*/*z* 389. Distinctive fragment ions

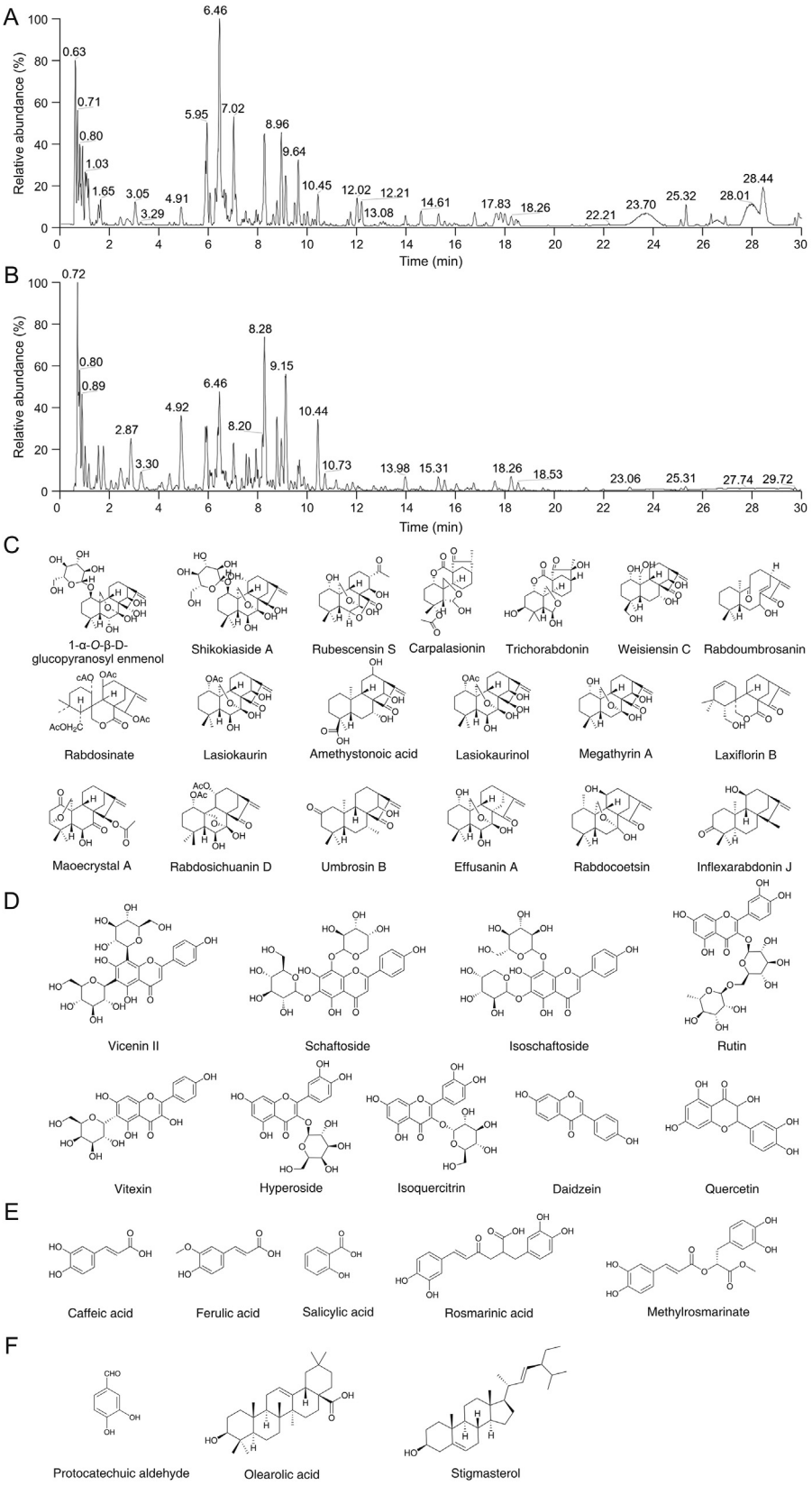

Fig. 1. Chemical analysis of *Rabdosia serra* (*R. serra*). Ultra performance liquid chromatography total ion chromatogram of *R. serra* in (A) positive and (B) negative ion modes. (C) *Ent*-kaurane diterpenoids, (D) flavonoids, (E) phenolic acids, and (F) steroids and other compounds identified in *R. serra*.

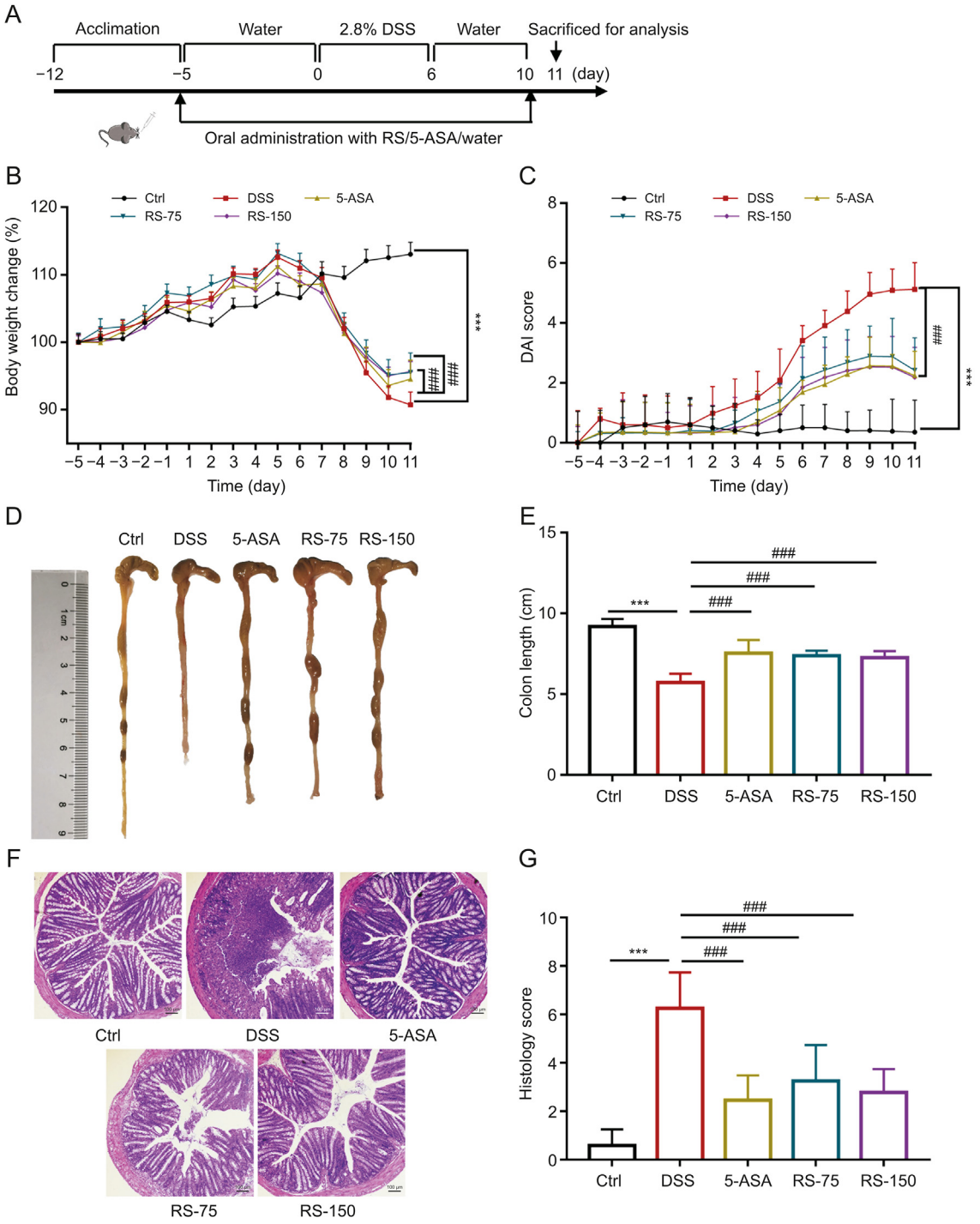

Fig. 2. *R. serra* showed strong efficacy in protecting against dextran sulfate sodium (DSS) salt-induced colitis in a mouse model. (A) Schematic illustration of the animal experimental procedure. (B) Body weight changes of each group were monitored daily and expressed as a percentage of initial weight. (C) Disease activity index (DAI) score. (D) Morphology of colons sampled from mice in each group. (E) Colon length. (F) Typical hematoxylin and eosin (H&E)-stained colonic sections. (G) Histopathological score. Ctrl: control group; DSS: DSS-induced colitis mice without other treatment; 5-ASA: DSS-induced colitis mice treated with 5-aminosalicylic acid (5-ASA) as a positive control; RS-75: DSS-induced colitis mice treated with *R. serra* at a dose of 75 mg/kg; RS-150: DSS-induced colitis mice treated with *R. serra* at a dose of 150 mg/kg. Results are presented as means ± SD, $n = 8$ for each group. $^{***}P < 0.001$, compared to control; $^{\#\#\#}P < 0.001$, compared to DSS.

at *m/z* 371 and 311 were obtained through a loss of H_2O ($[M-H-18\ Da]^+$) and AcOH ($[M-H-H_2O-78\ Da]^+$) from the deprotonated molecular ion $[M-H]^+$. Moreover, a typical fragment ion at *m/z* 269 was identified through the loss of 42 Da from the ion at *m/z* 311 ($[M-H-H_2O-AcOH-CH_2{=}CO]^+$).

Weisiensin C (**22**), the only 7,20-diepoxy-*ent*-kaurane found in *R. serra*, belongs to the C-20-oxygenated type. It was characterized from the tested ion ($[C_{20}H_{30}O_6-H]^-$) at *m/z* 365, and the characteristic fragment ions at *m/z* 347 ($[M-H-H_2O]^-$), 329 ($[M-H-2H_2O]^-$), and 321 ($[M-H-3H_2O]^-$) corresponded to the successive loss of neutral H_2O. Simultaneously, the typical fragment ion ($[M-H-H_2O-30\ Da]^-$) was formed, thereby producing a characteristic ion at *m/z* 307. A similar cleavage was observed for the fragment ion at *m/z* 273 ($[M-H-H_2O-CO_2]^-$) based on the fragment ion at *m/z* 303.

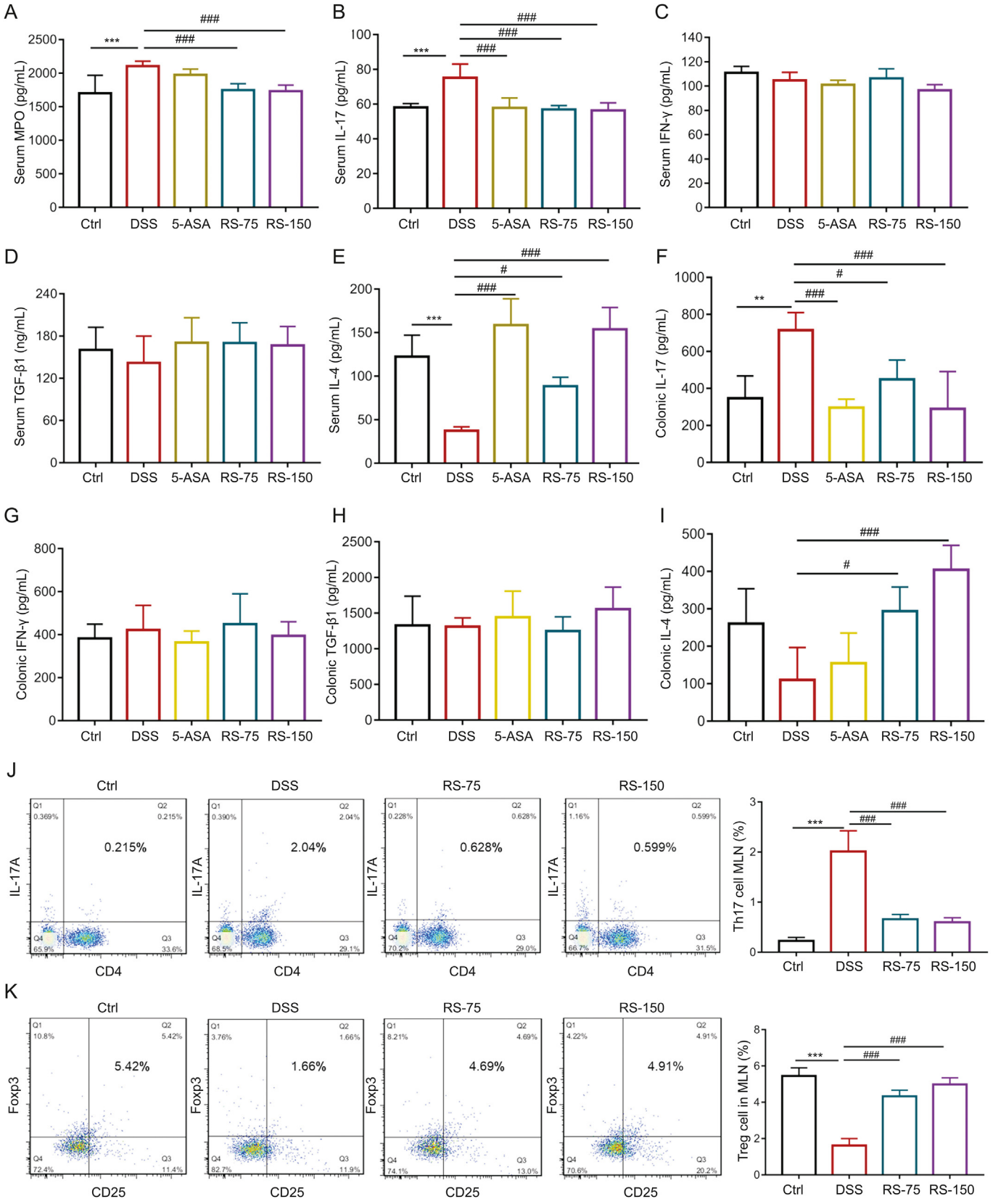

Fig. 3. *R. serra* alleviated dextran sulfate sodium (DSS)-induced inflammation. Serum levels of (A) myeloperoxidase (MPO), (B) interleukin (IL)-17, (C) interferon (IFN)-γ, (D) transforming growth factor (TGF)-β1, and (E) IL-4. Colonic levels of (F) IL-17, (G) IFN-γ, (H) TGF-β1, and (I) IL-4. Flow cytometry analysis of (J) T helper 17 (Th17) and (K) regulatory T (Treg) cells in mesenteric lymphoid nodes, with statistical data shown in the right panel. Th17 cells were assessed through CD4 and IL-17A. Treg cells were assessed through CD25 and Foxp3. Results are presented as means ± SD, $n = 8$ for each group. $^{**}P < 0.01$ and $^{***}P < 0.001$, compared to control; $^{\#}P < 0.05$ and $^{\#\#\#}P < 0.001$, compared to DSS. Ctrl: control; DSS: DSS-induced colitis mice without other treatment; 5-ASA: DSS-induced colitis mice treated with 5-aminosalicylic acid (5-ASA) as a positive control; RS-75: DSS-induced colitis mice treated with *R. serra* at a dose of 75 mg/kg; RS-150: DSS-induced colitis mice treated with *R. serra* at a dose of 150 mg/kg; MLN: mesenteric lymph nodes.

Four enmein type *ent*-kaurane diterpenoids were identified in the water extract of *R. serra*: compounds **17** (carpalasionin), **19** (trichorabdonin), **31** (rabdosichuanin D), and **42** (rabdoumbrosanin). Carpalasionin, as an example, produced a deprotonated molecular ion $[C_{22}H_{28}O_7–H]^-$ at *m/z* 419. The characteristic fragment ions at *m/z* 375 ($[M–H–CO_2]^-$) and 331 ($M–H–2CO_2]^-$) were obtained through a successive loss of the CO_2 fragment. Moreover, the typical fragment ion at *m/z* 263 occurred through the loss of CHOH based on the product ion at *m/z* 290.

Laxiflorin B, a spiro-lactone type *ent*-kaurane diterpenoid, exhibited an ion peak $[M–H]^-$ at *m/z* 343 with a distinctive deprotonated molecular ion $[C_{20}H_{24}O_5–H]^-$, which subsequently formed a typical ion at *m/z* 299 through the loss of a neutral fragment CO_2 and obtaining a fragment ion at *m/z* 281 ($[M–H–CO_2–H_2O]^-$). The identified fragment ion at *m/z* 255 ($[M–H–CO–CH_2O]^-$) was obtained through a subsequent loss of a CH_2O fragment based on the product ion at *m/z* 285.

Furthermore, nine flavonoids (Fig. 1D), namely, compounds **4** (vicenin II), **5** (schaftoside), **6** (isoschaftoside), **8** (rutin), **9** (vitexin), **10** (isoquercitrin), **11** (hyperoside), **18** (daidzein), and **21** (quercetin), were characterized and identified through comparisons with standards and MS/MS data. Vicenin II produced abundant $[C_{27}H_{30}O_{15}–H]^-$ ions at *m/z* 593. The characteristic fragment ions $[M–H–18\ Da]^-$, $[M–H–90\ Da]^-$, and $[M–H–C_3H_6O_3–30\ Da]^-$ were formed through a loss of H_2O, $C_3H_6O_3$, and CH_2O, respectively. Similar results were found for the fragment ions at *m/z* 383 $[M–H–2C_3H_6O_3–CH_2O]^-$ and *m/z* 353 $[M–H–2C_3H_6O_3–2CH_2O]^-$ based on the ion at *m/z* 473. Schaftoside and isoschaftoside are isomers that formed a mass of $[M+H]^+$ ions at *m/z* 565 in the ESI positive mode. A continual loss of a string of characteristic H_2O fragment ions from the hydroxyl groups was observed at *m/z* 547 ($[M+H–H_2O]^+$), 529 ($[M+H–2H_2O]^+$), and 511 ($[M+H–3H_2O]^+$). Moreover, typical fragment ions at *m/z* 499 ($[M+H–2H_2O–CH_2O]^+$) and 469 ($[M+H–2H_2O–2CH_2O]^+$) were formed through the cleavage of CH_2O based on the product ion *m/z* 529.

As shown in Fig. 1E, five phenolic acids, namely, compounds **2** (caffeic acid), **3** (ferulic acid), **12** (salicylic acid), **15** (rosmarinic acid), and **20** (methyl rosmarinate) were identified in the extract and characterized further. All phenolic acids were identified by comparison with reference standards.

Furthermore, three steroids and other compounds, including compounds **1** (protocatechuic aldehyde), **45** (oleanolic acid), and **46** (stigmasterol), were identified in the extract (Fig. 1F), among which oleanolic acid and stigmasterol were identified by comparison with the standards.

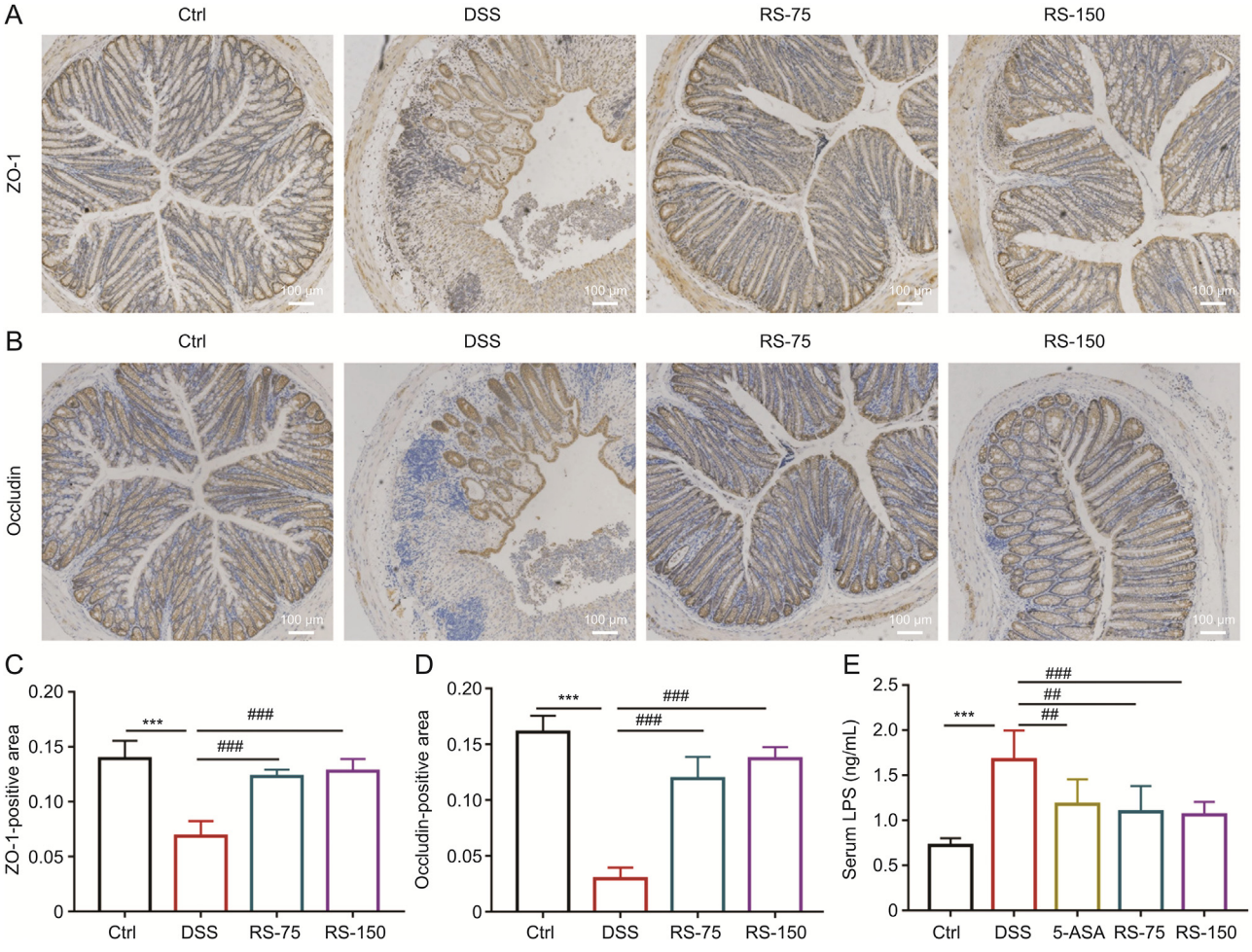

Fig. 4. *R. serra* preserved intestinal barrier function. Immunohistochemical (IHC) analysis to determine the expressions of (A) zonula occludens 1 (ZO-1) and (B) occluding proteins. The brown color between cells suggests positive expression of ZO-1 or occludin, and the blue staining represents the nucleus. (C) ZO-1 and (D) occludin quantified using ImageJ. (E) Serum lipopolysaccharide (LPS) levels in mice. Results are presented as means ± SD, $n = 8$ for each group. $^{***}P < 0.001$, compared to control; $^{\#}P < 0.05$, $^{\#\#}P < 0.01$ and $^{\#\#\#}P < 0.001$, compared to dextran sulfate sodium (DSS). Ctrl: control; DSS: DSS-induced colitis mice without other treatment; 5-ASA: DSS-induced colitis mice treated with 5-aminosalicylic acid (5-ASA) as a positive control; RS-75: DSS-induced colitis mice treated with *R. serra* at a dose of 75 mg/kg; RS-150: DSS-induced colitis mice treated with *R. serra* at a dose of 150 mg/kg.

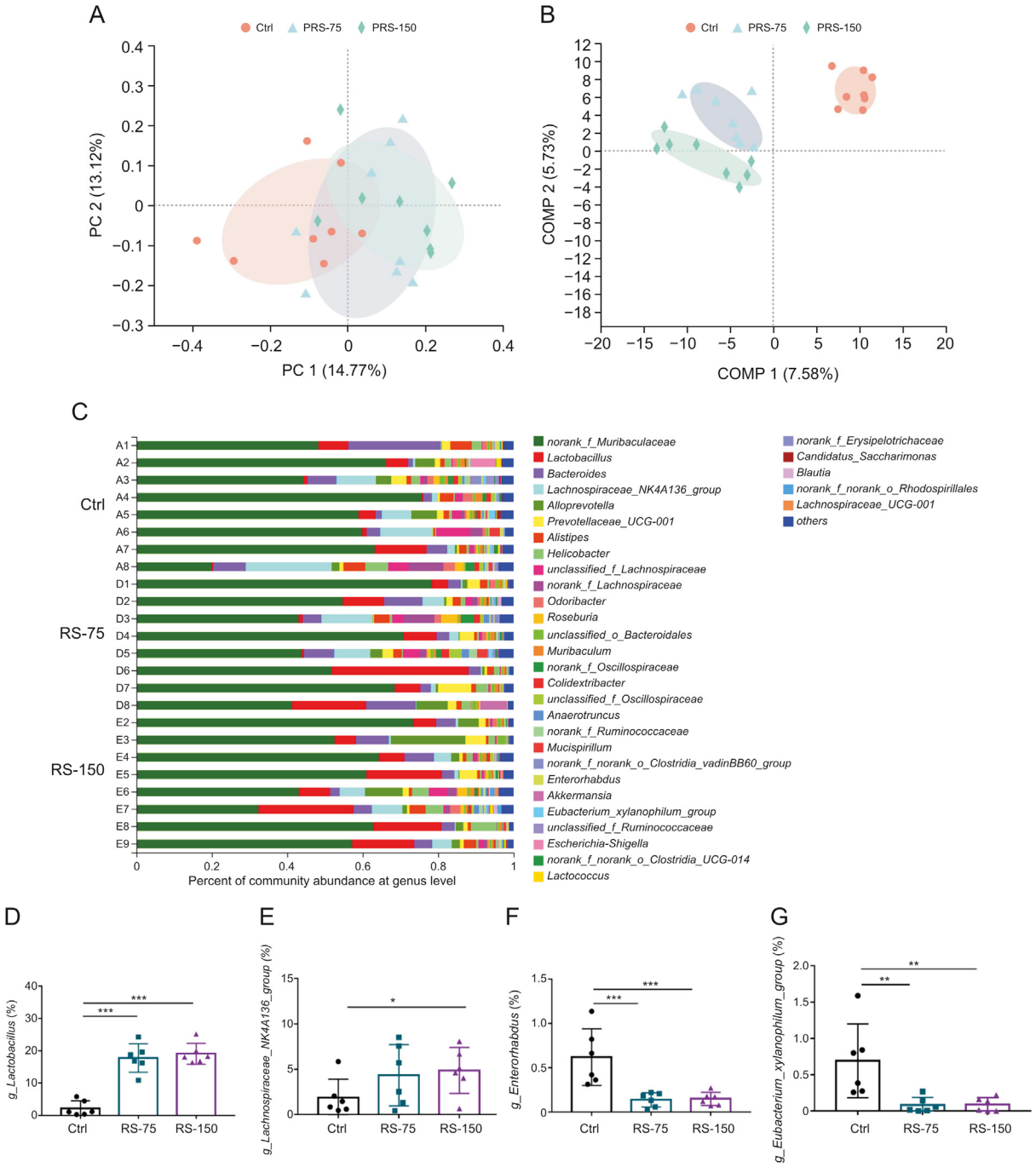

Fig. 5. Gut microbial diversity and structural changes in mice after pre-adminisatration with *R. serra* (PRS) before dextran sulfate sodium (DSS) treatment. (A) Principal coordinate analysis (PCoA) at the operational taxonomic unit (OTU) level; (B) partial least squares discriminant analysis (PLS-DA) at the OTU level; (C) community barplot analysis. Relative abundance of (D) *g_Lactobacillus*, (E) *g_Lachnospiraceae_NK4A136_group*, (F) *g_Enterorhabdus*, and (G) *g_Eubacterium_xylanophilum_group*. Results are presented as means ± SD, $n = 6–8$ for each group. $^{*}P < 0.05$, $^{**}P < 0.01$, and $^{***}P < 0.001$, compared to control. Ctrl: control; PRS-75: mice pre-administered with *R. serra* at a dose of 75 mg/kg before DSS treatment; RS-150: mice pre-administered with *R. serra* at a dose of 150 mg/kg before DSS treatment; COMP: component.

3.2. Antioxidant capacities of R. serra in vitro

Inflammation is closely linked to excessive oxidative stress. Medicinal herbs containing polyphenols can help increase antioxidant capacity and decrease oxidative stress [30]. Antioxidant enzymes such as superoxide dismutase (SOD) play a key role in protecting cells against oxidative stress. Glutathione (GSH), an antioxidant substance, also plays a critical role in balancing oxidative stress [31]. Therefore, in this study, the levels of SOD (Fig. S1A) and GSH (Fig. S1B) in H_2O_2-induced Caco-2 cells were determined to evaluate the antioxidant capacities of *R. serra* according to the methods described in the Supplementary material. Compared to untreated cells, SOD and GSH levels in Caco-2 cells were significantly decreased after H_2O_2 treatment, and *R. serra* treatment markedly alleviated the decrease in SOD and GSH levels in a concentration-dependent manner, indicating that *R. serra* can balance oxidative stress in vitro. A previous study reported that the antioxidant activities of Chinese herbs are related to their *ent*-kaurane diterpenoids, flavonoids, phenolic acids, and other phenolic

compounds [30]. Thus, the abovementioned findings indicate that *R. serra*, owing to its strong antioxidant activities, can be used as a potential antioxidant for the management of inflammatory diseases.

3.3. The water extract of R. serra ameliorated DSS-induced colitis in mice

A DSS-induced colitis mouse model was established, and the experimental procedure followed is presented in Fig. 2A. Compared to the control group, colitis mice (DSS group) showed severe clinical symptoms, including significant body weight loss (Fig. 2B), increased DAI scores (Fig. 2C), and shortened colon length (Figs. 2D and E). As shown in Fig. 2F, H&E staining revealed that the colonic tissue sections of the DSS group showed a marked increase in inflammatory cell infiltration, goblet and epithelial cell disappearance, crypt abscesses, muscle layer thickening and detachment, and even ulcer formation. Moreover, histopathological analysis revealed remarkable colonic injury in colon tissue (Fig. 2G). Strikingly, a pre-administration of the *R. serra* (PRS; the mice were administered with the water extract of *R. serra* before DSS was administered to induce colitis) water extract significantly protected the mice against DSS-mediated body weight loss, shortened colon length, and inhibited colon tissue damage. In this study, *R. serra* showed a preferable effect on alleviating the symptoms of DSS-induced colitis. When compared to the positive control 5-ASA, the first-line treatment option for IBD, *R. serra* treatment exhibited a similar efficacy in protecting against DSS-induced colitis [32]. Taken together, these results indicated that the water extract of *R. serra* could effectively ameliorate DSS-induced colitis in mice.

3.4. R. serra decreased the levels of inflammatory factors in colitis mice

Intestinal microbiome imbalance, severe mucosal damage, and inflammation are closely associated with dysregulation of the immune response and levels of pro-inflammatory factors, which could

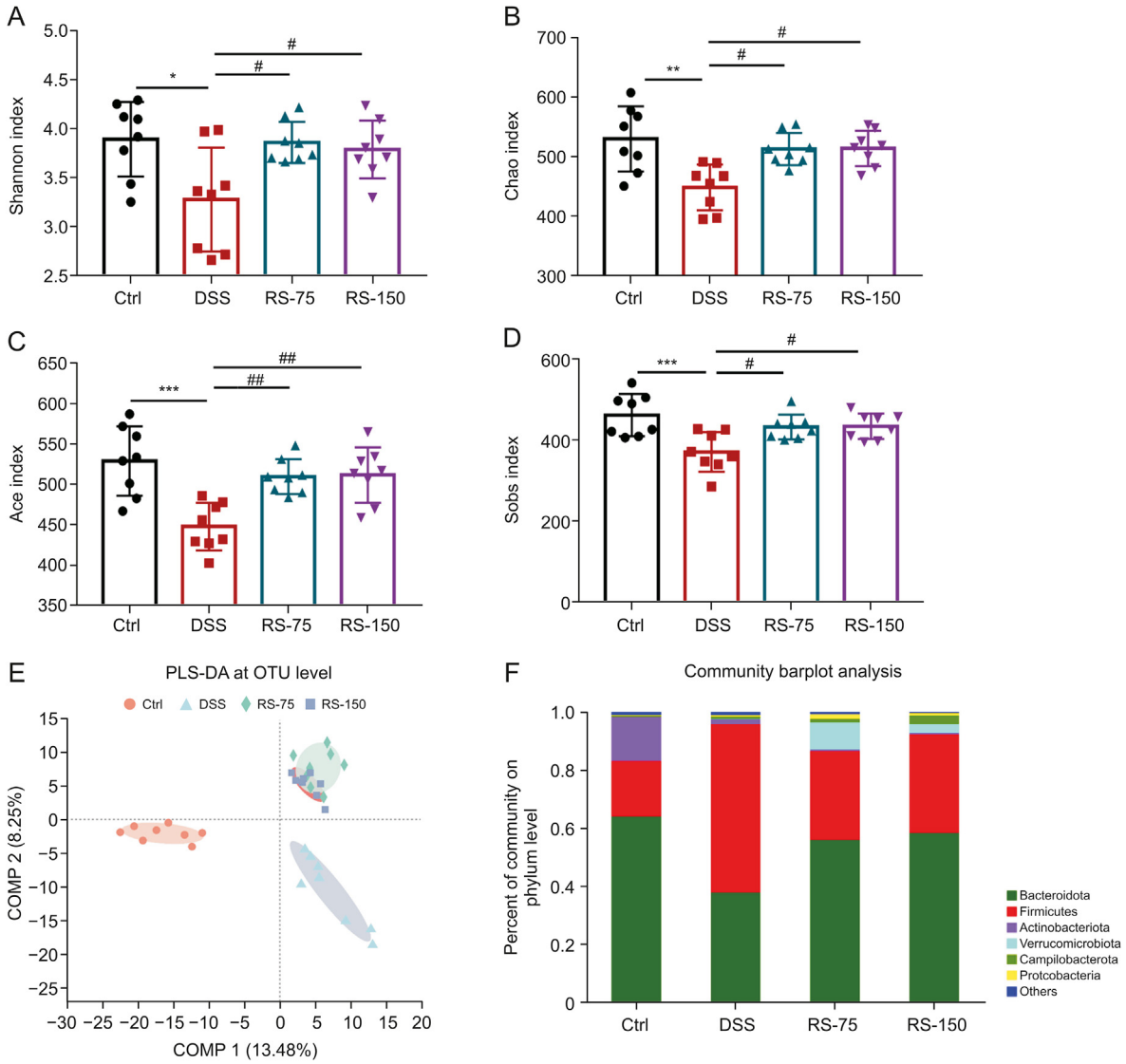

Fig. 6. *R. serra* modulated the gut microbiota diversity and structure in colitic mice. (A) Shannon index; (B) Chao index; (C) Ace index; (D) Sobs index; (E) partial least squares discriminant analysis (PLS-DA) at the operational taxonomic unit (OTU) level; and (F) abundance of bacteria at the phylum level. Results are presented as means ± SD, $n = 8$ for each group. $^{*}P < 0.05$, $^{**}P < 0.01$, and $^{***}P < 0.001$, compared to control; $^{\#}P < 0.05$ and $^{\#\#}P < 0.01$, compared to dextran sulfate sodium (DSS). Ctrl: control; DSS: DSS-induced colitis mice without other treatment; RS-75: DSS-induced colitis mice treated with *R. serra* at a dose of 75 mg/kg; RS-150: DSS-induced colitis mice treated with *R. serra* at a dose of 150 mg/kg; COMP: component.

exacerbate IBD inflammation [7]. The levels of pro- and anti-inflammatory factors in both serum and colonic tissue were evaluated to explore the anti-inflammatory effect of *R. serra* on acute intestinal inflammation in DSS-induced colitis mice. Myeloperoxidase (MPO), a glycosylated enzyme, is a marker for inflammation, oxidative damage, and mucosal injury status in patients with IBD

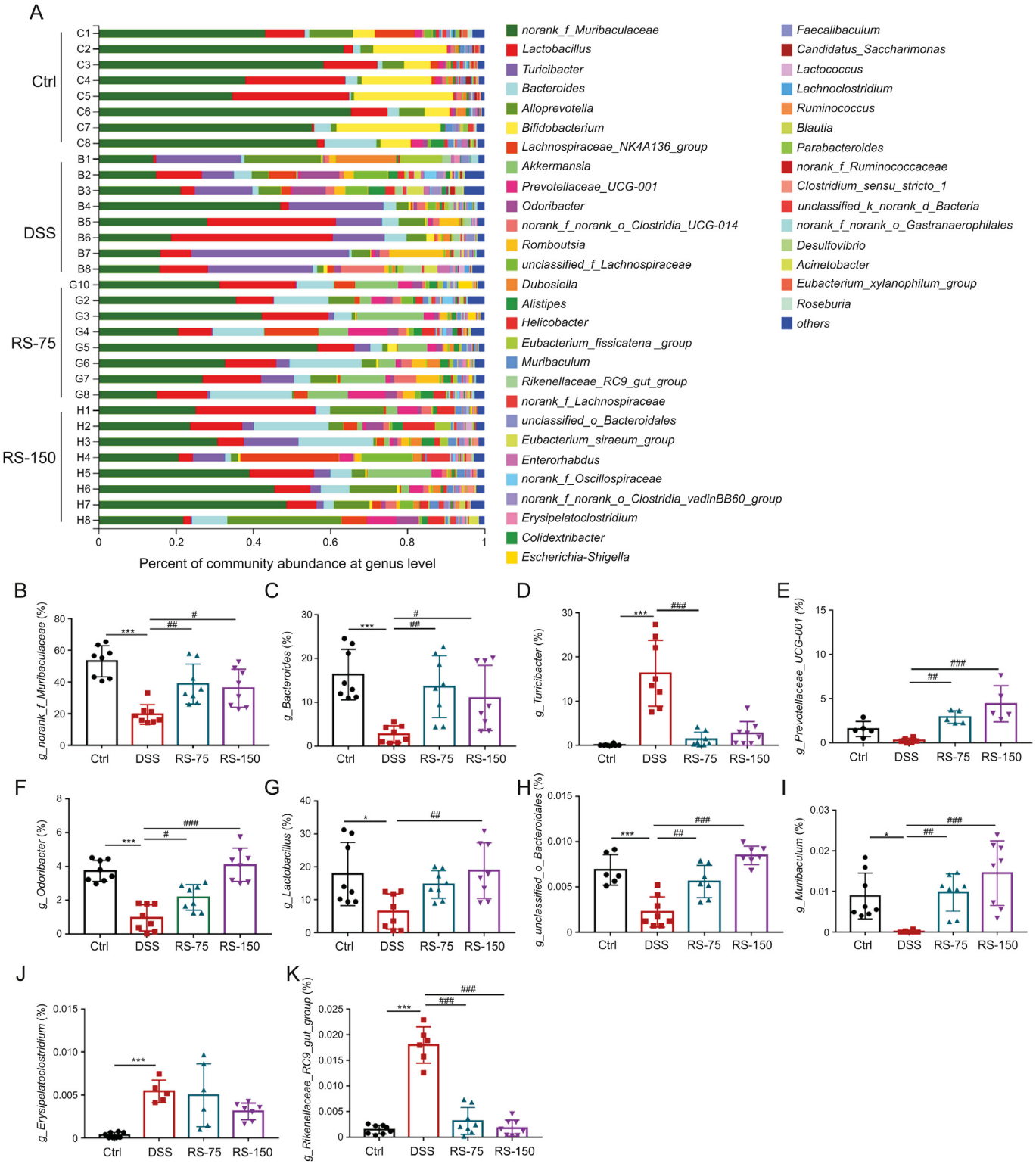

Fig. 7. Gut microbial alterations at the genus level. (A) Community barplot analysis at the genus level. Relative abundance of (B) g_*norank_f_Muribaculaceae*, (C) g_*Bacteroides*, (D) g_*Turicibacter*, (E) g_*Prevotellaceae_UGC-001*, (F) g_*Odoribacter*, (G) g_*Lactobacillus*, (H) g_*unclassified_o_Bacteroidales*, (I) g_*Muribaculum*, (J) g_*Erysipelatoclostridium*, and (K) g_*Rikenellaceae_RC9_gut_group*. Results are presented as means ± SD, $n = 6–8$ for each group. $^{*}P < 0.05$, $^{**}P < 0.01$, and $^{***}P < 0.001$, compared to control; $^{\#}P < 0.05$, $^{\#\#}P < 0.01$, and $^{\#\#\#}P < 0.001$, compared to dextran sulfate sodium (DSS). Ctrl: control; DSS: DSS-induced colitis mice without other treatment; RS-75: DSS-induced colitis mice treated with *R. serra* at a dose of 75 mg/kg; RS-150: DSS-induced colitis mice treated with *R. serra* at a dose of 150 mg/kg.

[33]. Fig. 3A shows the serum MPO level of each treatment group. MPO level was significantly increased in the DSS group and was significantly decreased by *R. serra* treatment. Moreover, the pro-inflammatory factors IFN-γ and IL-17 are markers for inflammation that are closely associated with the progression of IBD. As shown in Figs. 3B-I, *R. serra* treatment markedly decreased the levels of IL-17 and IFN-γ in the serum and colonic tissue and increased the levels of anti-inflammatory factors IL-4 and TGF-β1. Similar effects were observed in the 5-ASA group. All these results suggested that *R. serra* alleviated intestinal inflammation in DSS-induced colitis mice by decreasing the levels of pro-inflammatory factors and promoting the expressions of anti-inflammatory factors.

It has been proven that Th17 and Treg cells, differentiated from $CD4^+$ T cells, are closely related to the occurrence, development, and prognosis of IBD [34]. Th17 cells play a pro-inflammatory role by secreting the pro-inflammatory factors IL-21, IL-17, IFN-γ, and IL-22, while Treg cells play important anti-inflammatory and immunoregulatory roles by producing the anti-inflammatory factors IL-4, IL-10, and TGF-β [35,36]. A balance between Th17 and Treg cells is required to regulate the intestinal immune responses [36]. In this study, the effect of the water extract of *R. serra* on Th17/Treg cell balance in DSS-induced colitis mice was evaluated (Figs. 3J and K). *R. serra* treatment significantly decreased the percentage of $IL17A^+$ $CD4^+$ Th17 cells in MLNs and increased that of $CD25^+$ $Foxp3^+$ Treg cells. These values were consistent with the levels of inflammatory factors evaluated in the serum and colon of colitis mice.

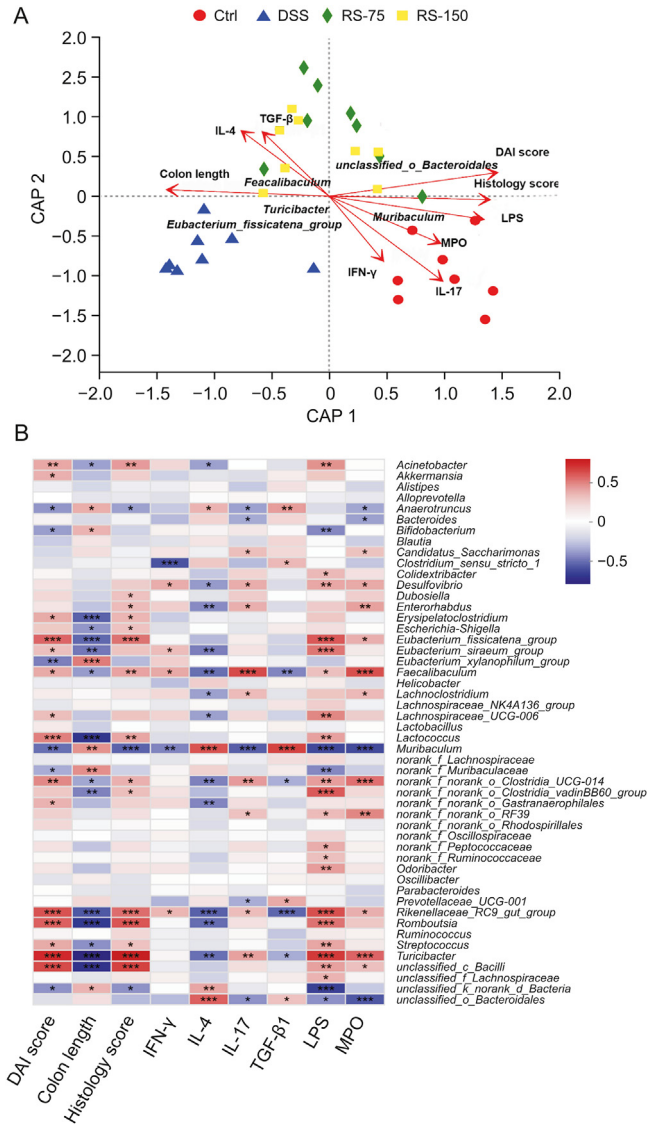

Fig. 8. Correlation analysis. (A) Distance-based redundancy analysis. (B) Spearman correlation heatmap. Results are presented as means ± SD, $n = 6–8$ for each group. $^*P < 0.05$, $^{**}P < 0.01$ and $^{***}P < 0.001$. DAI: disease activity index; IFN: interferon; IL: interleukin; TGF: transforming growth factor; LPS: lipopolysaccharide; MPO: myeloperoxidase; Ctrl: control; DSS: dextran sulfate sodium (DSS)-induced colitis mice without other treatment; RS-75: DSS-induced colitis mice treated with *R. serra* at a dose of 75 mg/kg; RS-150: DSS-induced colitis mice treated with *R. serra* at a dose of 150 mg/kg.

3.5. *R. serra* preserved intestinal barrier function and reduced gut permeability

Previous studies have reported that intestinal epithelial layer injury in the gastrointestinal tract is one of the symptoms of IBD [3]. Therefore, the integrity of intestinal barrier function is critical for maintaining gut health. Tight junction proteins, including ZO-1, claudins, occludin, and tricellulin, are directly responsible for intestinal barrier function and can decrease gut permeability and defense against pathogenic molecules such as LPS [12,37,38]. Therefore, the expressions of occludin and ZO-1 in colonic tissue were evaluated through IHC analysis (Figs. 4A–D). As shown in Figs. 4A and B, mice in the DSS group exhibited deteriorated intestinal epithelial layer with a decrease in occludin and ZO-1 expressions, which were markedly improved by *R. serra* treatment.

The microbial endotoxin LPS is an indicator of gut permeability. Because of the disruption of the gut mucosa, LPS is transported to the systemic circulation and continuously stimulates the immune system [38]. As shown in Fig. 4E, serum LPS levels, which were increased by DSS, were significantly decreased by *R. serra* in mice. Furthermore, tight junction proteins can prevent the permeation of LPS from the intestinal tract into the blood [39]. Hence, the increased levels of LPS in the DSS group might be associated with the decreased expressions of ZO-1 and occludin. As *R. serra* can ameliorate DSS-mediated changes in the levels of ZO-1, occludin, and LPS, it might play a key role in repairing the intestinal barrier and reducing the level of external endotoxins.

3.6. *R. serra* alleviated DSS-induced gut dysbiosis

Increasing evidence has proven that the intestinal flora is closely associated with the pathogenesis of IBD [13]. The gut microbiota plays a key role in defending against pathogens and regulating immune responses. However, alterations of the intestinal microbiome can drive the activation and differentiation of immune cells [4,7]. Modulating the structure of the gut microbiota can be a promising therapy for IBD. To determine whether *R. serra* can regulate the diversity and structural composition of the intestinal microbiome, we studied mouse fecal bacterial DNA by performing high-throughput gene sequencing analysis of 16S rRNA.

First, the gut microbial composition was evaluated before DSS induction in mice. Fecal specimens were collected after one week of oral pretreatment with *R. serra* at a dose of 75 and 150 mg/kg in normal C57BL/6J mice. Compared with the control group, mice in the PRS group showed similar richness and diversity of the gut microbiota in terms of the OTU level, which was determined by analyzing the α-diversity estimators (Chao, Shannon, Ace, and Sobs indices) (Figs. S2A–D). Additionally, a β-diversity analysis of the OTU level and PCoA and PLS-DA results were performed to evaluate the structural changes of the gut microbiota. As shown in Figs. 5A and B, a significant separation between the microbiota of

the PRS group and that of the control group was observed. Furthermore, a community barplot analysis at the phylum level indicated that Firmicutes, Bacteroidetes, and Campilobacterota were the dominant members of the gut microbiota (Fig. S2E and F). Meanwhile, *Lachnospiraceae_NK4A136_group* and *Lactobacillus* were significantly increased, while *Enterorhabdus* and *Eubacterium_xylanophilum_group* were significantly decreased (Figs. 5D–G) through pretreatment with *R. serra*. *Lachnospiraceae_NK4A136_group* and *Lactobacillus* were beneficial microbial species [4,7], while *Enterorhabdus* and *Eubacterium_xylanophilum_group* were found to be positively related to metabolic diseases and colon cancer [40,41]. It has been reported that the *Lachnospiraceae_NK4A136_group* plays an important role in anti-inflammation by alleviating the symptoms of colonic inflammation and inhibiting the expressions of pro-inflammatory factors such as TNF-α, IL-6, and IL-12 [41–43]. Generally, *Lactobacillus* can protect against pathogen colonization in the gut by creating a barrier [42]. In conclusion, although there was no significant variation in the richness and diversity of the gut microbiota between mice pretreated with *R. serra* and control mice, *R. serra* increased the relative abundance of beneficial bacteria.

Subsequently, fecal specimens of the DSS-induced colitis mice were collected for 16S rRNA analysis after *R. serra* treatment. The results showed that DSS treatment significantly reduced the Shannon (Fig. 6A), Chao (Fig. 6B), Ace (Fig. 6C), and Sobs (Fig. 6D) indices, indicating that the richness and diversity of the gut

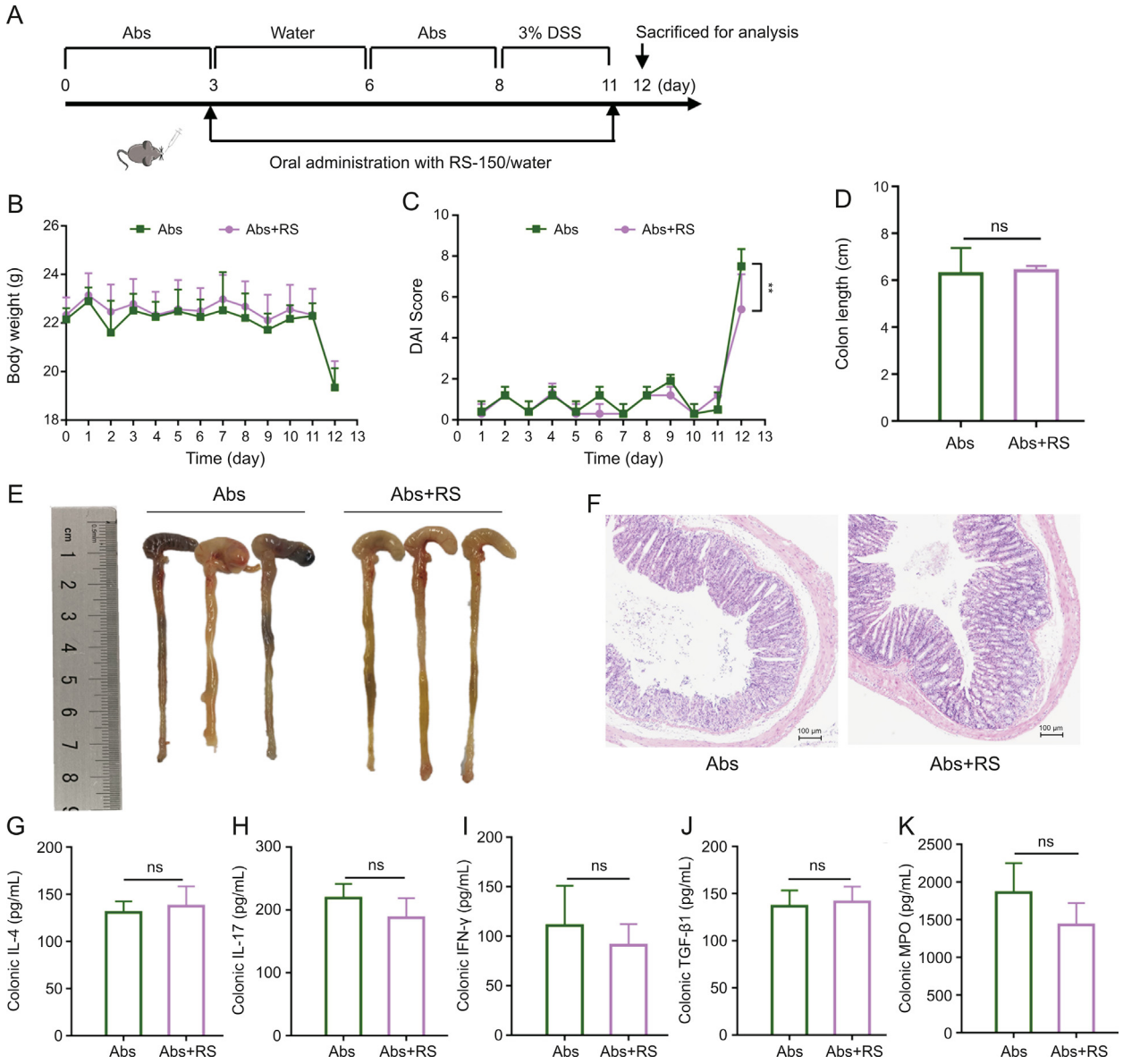

Fig. 9. Therapeutic effect of *R. serra* on dextran sulfate sodium (DSS)-induced colitis mice was microbiota dependent. (A) Schematic illustration of the animal experiment design. C57BL/6J mice were pretreated with a broad-spectrum oral antibiotic (Abs) cocktail (100 mg/Kg of vancomycin, 200 mg/Kg of ampicillin, 200 mg/Kg of metronidazole, and 200 mg/Kg of neomycin sulfate) at days 0–3 and 6–8 and then administered with 3% DSS (*m*/*V*) for 4 days (days 8–11). The Abs and Abs + *R. serra* (RS) group were orally administered water and *R. serra* (150 mg/kg/day) (RS-150) from day 3 to day 11. (B) Body weight changes of each group were monitored daily and expressed as a percentage of initial weight. (C) Disease activity index (DAI) score. (D) Colon length. (E) Morphology of colons. (F) Typical hematoxylin and eosin (H&E) stained colon tissue sections. Colonic levels of (G) interleukin (IL)-4, (H) IL-17, (I) interferon (IFN)-γ, (J) transforming growth factor (TGF)-β1, and (K) myeloperoxidase (MPO). Abs group: Abs-treated mice administered with water; Abs + RS: Abs-treated mice administered with *R. serra* extract. *P* values were analyzed using unpaired *t*-tests. $^{**}P < 0.01$; ns: not significant.

microbiota were decreased. With *R. serra* treatment, these indices were increased, suggesting a recovery of intestinal microbial richness and diversity. Furthermore, a PLS-DA plot of the OTU level revealed that the *R. serra*-treated group was separated from the DSS group moving toward the control group based on the first two components (Fig. 6E). It thus suggests that *R. serra* can at least partially recover microbial diversity and composition in colitis.

Fig. 6F shows a community barplot analysis of the gut microbiota at the phylum level. The abundance of Bacteroidota was much lower in the DSS group than in the control group, but its level was recovered with *R. serra* treatment. In contrast, compared with the control group, the abundance of Firmicutes was increased in the DSS group and was recovered after *R. serra* treatment.

As shown in Fig. 7A, remarkable alterations in the gut microbiota at the genus level were observed. The relative abundance of *norank_f_Muribaculaceae* (Fig. 7B), *Bacteroides* (Fig. 7C), *Prevotellaceae_UCG-001* (Fig. 7E), *Odoribacter* (Fig. 7F), *Lactobacillus* (Fig. 7G), *unclassified_o_Bacteroidales* (Fig. 7H), and *Muribaculum* (Fig. 7I) were decreased by DSS treatment, while that of *Turicibater* (Fig. 7D) and *Rikenellaceae_RC9_gut_group* (Fig. 7K) were increased. The relative aboundance of g_*Erysipelatoclostridium* was not significantly different between DSS and RS groups (Fig. 7J). *R. serra* treatment was able to normalize the ratio of these bacterial genus. Moreover, as revealed by the community barplot analysis at the genus level, the family *Muribaculaceae*, which are propionate-producing intestinal bacteria, were predominant members of the gut microbiota in healthy mice. It has been proven that propionate, a short-chain fatty acid, can improve intestinal barrier function and reduce oxidative stress and inflammation in DSS-induced colitis [44]. Moreover, *Lactobacillus* and *Bacteroides* are also considered to exhibit anti-inflammatory activity and promote recovery of the intestinal mucosa [12,13,45]. *Lactobacillus* can reduce the expressions of pro-inflammatory factors, modulate oxidative stress, and prevent metabolic disorders [46,47]. We found that *R. serra* played a role in restoring the balance of the gut microbiota by elevating the abundance of *norank_f_Muribaculaceae*, *Lactobacillus*, *Prevotellaceae_UCG-001*, and *Bacteroides*.

3.7. Results of the Db-RDA analysis and Spearman correlation

To test whether the therapeutic effect of *R. serra* on DSS-induced colitis mice is associated with inflammatory factors, immune cells, and the gut microbiota, Db-RDA and Spearman correlation heatmap analyses were performed (Fig. 8). Db-RDA analysis revealed that *R. serra* treatment was positively correlated with histology score, DAI score, colon length, and the anti-inflammatory factors IL-4 and TGF-β. Furthermore, Spearman correlation heatmap analysis revealed that DAI score and histology score were highly correlated with *Turicibacter*, *unclassified_c_Bacilli*, *Romboutsia*, *Rikenellaceae_RC9_gut_group*, *Lactococcus*, and *Eubacteriun_fissicatena_group*. The anti-inflammatory factors IL-4 and TGF-β1 were significantly correlated with *unclassified_o_Bacteroidales* and *Muribaculum*, while the pro-inflammatory factors IFN-γ and IL-17 were correlated with *Rikenellaceae_RC9_gut group* and *Feacalibaculum*. Indeed, *Feacalibaculum* has been proven to be able to induce inflammation by destroying the intestinal barrier [48]. Previous studies have reported that the *Rikenellaceae_RC9_gut group* can contribute to intestinal inflammation by increasing intestinal permeability and oxidative stress and impacting energy metabolism [49,50]. Moreover, there was a significant correlation between LPS and MPO with *Utriculate*, *unclassified_c_Bacilli*, *Rikenellaceae_RC9_gut_group*, *norank_f_norank_o_Clostridia_UCG-014*, *Faecalibaculum*, and *Eubacterium_fissicatena_group*.

Above all, *R. serra* modulated the gut microbiota in DSS-induced mice by restoring its richness and diversity, increasing the abundance of beneficial bacteria, including *Muribaculaceae, Bacteroides, Lactobacillus*, *Lachnospiraceae_NK4A136*_group, and *Prevotellaceae_UCG-001*, and decreasing the abundance of pathogenic bacteria, including *Turicibacter*, *Eubacterium_fissicatena_group*, and *Eubacterium_xylanophilum_group*.

3.8. R. serra ameliorated DSS-induced colitis in mice in a microbiota-dependent manner

To further confirm whether the effect of *R. serra* on DSS-induced colitis mice is microbiota dependent, we pretreated the C57BL/6 mice with a broad-spectrum oral antibiotic (Abs) cocktail to disrupt the intestinal microbiome before administering them with 3% DSS to induce acute colitis (Fig. 9A). The *R. serra*-untreated group was treated with an antibiotic cocktail (Abs group) as a control. Body weight changes and DAI score were recorded daily. Compared with the Abs group, antibiotic cocktail and *R. serra* treatment (Abs + RS group) did not significantly ameliorate the symptoms of DSS-induced colitis, manifested by similar body weight changes (Fig. 9B) and colon length (Figs. 9D and E). H&E staining of both groups revealed a partial crypt architecture disruption, inflammatory cell infiltration, and goblet cell loss (Fig. 9F). However, the DAI score of the Abs + RS group on the last day was lower than that of the Abs group (Fig. 9C). Moreover, determination of the levels of pro- and anti-inflammatory factors in colonic tissue (Figs. 9G–K) revealed that the anti-inflammatory effect of *R. serra* was abolished in the absence of interaction with the gut microbiota. These results indicate that *R. serra* can alleviate DSS-induced colitis by modulating the gut microbiome.

4. Conclusion

In conclusion, *R. serra* alleviated DSS-induced colitis in a gut microbiota-dependent manner. A total of 46 compounds, consisting of 19 *ent*-kaurane diterpenoids, 9 flavonoids, 5 phenolic acids, 3 steroids, and 10 other compounds, were identified in the water extract of *R. serra* using UPLC-LTQ-Orbitrap-MS. Additionally, in a DSS-induced colitis mouse model, *R. serra* was shown to significantly improve colon length, upregulate the anti-inflammatory factors MPO, IL-17, IFN-γ, and LPS, downregulate the pro-inflammatory factors IL-4 and TGF-β, and restore Th17/Treg cell imbalance. *R. serra* could also preserve intestinal barrier function by increasing the level of the tight junction proteins ZO-1 and occludin in colonic tissue. Furthermore, *R. serra* altered the gut microbiota composition by increasing bacterial richness and diversity, increasing the abundance of beneficial bacteria (*Muribaculaceae, Bacteroides, Lactobacillus*, *Lachnospiraceae_NK4A136_group,* and *Prevotellaceae_UCG-001*), and decreasing the abundance of pathogenic bacteria (*Turicibacter, Eubacterium_fissicatena_group*, and *Eubacterium_xylanophilum_group*), which was further confirmed by the depletion of the gut microbiota.

CRediT author statement

Hongyi Li: Investigation, Data curation, Writing - Original draft preparation; **Yi Wang:** Methodology, Investigation, Data curation; **Shumin Shao** and **Hui Yu:** Resources; **Deqin Wang** and **Chuyuan Li:** Formal analysis, Data curation; **Qin Yuan** and **Wen Liu:** Investigation, Formal analysis, Data curation; **Jiliang Cao:** Investigation, Data curation; **Xiaojuan Wang:** Writing - Reviewing and Editing; **Haibiao Guo:** Resources; **Xu Wu** and **Shengpeng Wang:**

Conceptualization, Supervision, Writing - Reviewing and Editing.

Declaration of competing interest

The authors declare that there are no conflicts of interest.

Acknowledgments

This work was supported by the Science and Technology Development Fund of Macao, China (File No.: 0151/2020/A3), Key Area Research and Development Program of Guangdong Province, China (Grant No.: 2020B1111110003), the Research Fund of the University of Macau, Macao, China (File No.: MYRG2020-00141-ICMS), and the Research Fund of Southwest Medical University, China (Grant No.: 2021ZKZD017).

Appendix A. Supplementary data

Supplementary data to this article can be found online at https://doi.org/10.1016/j.jpha.2022.08.001.

References

[1] A. Kaser, S. Zeissig, R.S. Blumberg, Inflammatory bowel disease, Annu. Rev. Immunol. 28 (2010) 573–621.
[2] N.T. Ventham, N.A. Kennedy, E.R. Nimmo, et al., Beyond gene discovery in inflammatory bowel disease: The emerging role of epigenetics, Gastroenterology 145 (2013) 293–308.
[3] Y. Lee, K. Sugihara, M.G. Gillilland 3rd, et al., Hyaluronic acid-bilirubin nanomedicine for targeted modulation of dysregulated intestinal barrier, microbiome and immune responses in colitis, Nat. Mater. 19 (2020) 118–126.
[4] E.A. Franzosa, A. Sirota-Madi, J. Avila-Pacheco, et al., Gut microbiome structure and metabolic activity in inflammatory bowel disease, Nat. Microbiol. 4 (2019) 293–305.
[5] G.J. Britton, E.J. Contijoch, M.P. Spindler, et al., Defined microbiota transplant restores Th17/RORγt^{+} regulatory T cell balance in mice colonized with inflammatory bowel disease microbiotas, Proc. Natl. Acad. Sci. U S A 117 (2020) 21536–21545.
[6] T.S. Dong, A. Gupta, Influence of early life, diet, and the environment on the microbiome, Clin. Gastroenterol. Hepatol. 17 (2019) 231–242.
[7] W. Zhang, C. Cheng, Q. Han, et al., *Flos Abelmoschus manihot* extract attenuates DSS-induced colitis by regulating gut microbiota and Th17/Treg balance, Biomed. Pharmacother. 117 (2019), 109162.
[8] S. Khan, S. Waliullah, V. Godfrey, et al., Dietary simple sugars alter microbial ecology in the gut and promote colitis in mice, Sci. Transl. Med. 12 (2020), eaay6218.
[9] K.L. Glassner, B.P. Abraham, E.M.M. Quigley, The microbiome and inflammatory bowel disease, J. Allergy Clin. Immunol. 145 (2020) 16–27.
[10] Á. Rol, T. Todorovski, P. Martin-Malpartida, et al., Structure-based design of a Cortistatin analogue with immunomodulatory activity in models of inflammatory bowel disease, Nat. Commun. 12 (2021), 1869.
[11] C.N. Bernstein, M. Fried, J.H. Krabshuis, et al., World gastroenterology organization practice guidelines for the diagnosis and management of IBD in 2010, Inflamm. Bowel Dis. 16 (2010) 112–124.
[12] Y. Wang, H. Tao, H. Huang, et al., The dietary supplement *Rhodiola crenulata* extract alleviates dextran sulfate sodium-induced colitis in mice through anti-inflammation, mediating gut barrier integrity and reshaping the gut microbiome, Food Funct. 12 (2021) 3142–3158.
[13] Y.-B. Zhong, Z.-P. Kang, M.-X. Wang, et al., Curcumin ameliorated dextran sulfate sodium-induced colitis via regulating the homeostasis of DCs and Treg and improving the composition of the gut microbiota, J. Funct. Foods 86 (2021), 104716.
[14] T.K. Motawi, S.M. Rizk, A.H. Shehata, Effects of curcumin and *Ginkgo biloba* on matrix metalloproteinases gene expression and other biomarkers of inflammatory bowel disease, J. Physiol. Biochem. 68 (2012) 529–539.
[15] W. Zhou, H. Xie, P. Wu, et al., Abietane diterpenoids from *Isodon lophanthoides* var. *graciliflorus* and their cytotoxicity, Food Chem 136 (2013) 1110–1116.
[16] W. Zhou, H. Xie, X. Xu, et al., Phenolic constituents from *Isodon lophanthoides* var. *graciliflorus* and their antioxidant and antibacterial activities, J. Funct. Foods 6 (2014) 492–498.
[17] Y. Du, P. Liu, H. Zhu, et al., A sensitive analysis method for 7 diterpenoids in rat plasma by liquid chromatography-electrospray ionization mass spectrometry and its application to pharmacokinetic study of *Isodon serra* extract, J. Chromatogr. A 1218 (2011) 7771–7780.
[18] L.L. Wong, Z. Liang, H. Chen, et al., Rapid differentiation of Xihuangcao from the three *Isodon* species by UPLC-ESI-QTOF-MS/MS and chemometrics analysis, Chin. Med. 11 (2016), 48.
[19] J. Wan, M. Liu, H.-Y. Jiang, et al., Bioactive *ent*-kaurane diterpenoids from *Isodon serra*, Phytochemistry 130 (2016) 244–251.
[20] Y. Liang, H. Xie, P. Wu, et al., Podocarpane, isopimarane, and abietane diterpenoids from *Isodon lophanthoides* var. *graciliflorus*, Food Chem 136 (2013) 1177–1182.
[21] Y. Zhao, S.-X. Huang, L.-B. Yang, et al., Cytotoxic *ent*-kaurane diterpenoids from *Isodon henryi*, Planta Med. 75 (2009) 65–69.
[22] D. Duan, Y. Wang, X. Jin, et al., Natural diterpenoid eriocalyxin B covalently modifies glutathione and selectively inhibits thioredoxin reductase inducing potent oxidative stress-mediated apoptosis in colorectal carcinoma RKO cells, Free Radic. Biol. Med. 177 (2021) 15–23.
[23] Y.-F. Guan, X.-J. Liu, X.-J. Pang, et al., Recent progress of oridonin and its derivatives for cancer therapy and drug resistance, Med. Chem. Res. 30 (2021) 1795–1821.
[24] Q.J. Wu, X.C. Zheng, T. Wang, et al., Effect of dietary oridonin supplementation on growth performance, gut health, and immune response of broilers infected with *Salmonella pullorum*, Ir. Vet. J. 71 (2018), 16.
[25] J. Cao, T. Lei, S. Wu, et al., Development of a comprehensive method combining UHPLC-CAD fingerprint, multi-components quantitative analysis for quality evaluation of Zishen Yutai Pills: A step towards quality control of Chinese patent medicine, J. Pharm. Biomed. Anal. 191 (2020), 113570.
[26] J.L. Cao, L.J. Ma, S.P. Wang, et al., Comprehensively qualitative and quantitative analysis of ginsenosides in *Panax notoginseng* leaves by online two-dimensional liquid chromatography coupled to hybrid linear ion trap Orbitrap mass spectrometry with deeply optimized dilution and modulation system, Anal. Chimica Acta 1079 (2019) 237–251.
[27] S. Huang, W. Hu, S. Zeng, et al., Comparative transcriptome analysis and simple sequence repeat marker development for two closely related *Isodon* species used as 'Xihuangcao' herbs, Trop. J. Pharm. Res. 18 (2019) 75–84.
[28] J. Wan, H.Y. Jiang, J.W. Tang, et al., *Ent*-abietanoids isolated from *Isodon serra*, Molecules 22 (2017), 309.
[29] F.L. Yan, L.B. Zhang, J.X. Zhang, et al., Two new diterpenoids from *Isodon serra*, Chin. Chem. Lett. 18 (2007) 1383–1385.
[30] A. Deledda, G. Annunziata, G.C. Tenore, et al., Diet-derived antioxidants and their role in inflammation, obesity and gut microbiota modulation, Antioxidants (Basel) 10 (2021), 708.
[31] Q. Zheng, J. Chen, Y. Yuan, et al., Structural characterization, antioxidant, and anti-inflammatory activity of polysaccharides from Plumula Nelumbinis, Int. J. Biol. Macromol. 212 (2022) 111–122.
[32] C. Le Berre, G. Roda, M. Nedeljkovic Protic, et al., Modern use of 5-aminosalicylic acid compounds for ulcerative colitis, Expert Opin. Biol. Ther. 20 (2020) 363–378.
[33] B. Chami, N.J.J. Martin, J.M. Dennis, et al., Myeloperoxidase in the inflamed colon: A novel target for treating inflammatory bowel disease, Arch. Biochem. Biophys. 645 (2018) 61–71.
[34] A. Ueno, L. Jeffery, T. Kobayashi, et al., Th17 plasticity and its relevance to inflammatory bowel disease, J. Autoimmun. 87 (2018) 38–49.
[35] J.-B. Yan, M.-M. Luo, Z.-Y. Chen, et al., The function and role of the Th17/Treg cell balance in inflammatory bowel disease, J Immunol. Res. 2020 (2020), 8813558.
[36] Y. Chang, L. Zhai, J. Peng, et al., Phytochemicals as regulators of Th17/Treg balance in inflammatory bowel diseases, Biomed. Pharmacother. 141 (2021), 111931.
[37] W.T. Kuo, L. Shen, L. Zuo, et al., Inflammation-induced occludin downregulation limits epithelial apoptosis by suppressing caspase-3 expression, Gastroenterology 157 (2019) 1323–1337.
[38] J. Liu, J. Cai, P. Fan, et al., The abilities of salidroside on ameliorating inflammation, skewing the imbalanced nucleotide oligomerization domain-like receptor family pyrin domain containing 3/autophagy, and maintaining intestinal barrier are profitable in colitis, Front. Pharmacol. 10 (2019), 1385.
[39] E.J. Park, A.B. Thomson, M.T. Clandinin, Protection of intestinal occludin tight junction protein by dietary gangliosides in lipopolysaccharide-induced acute inflammation, J. Pediatr. Gastroenterol. Nutr. 50 (2010) 321–328.
[40] C.J. Meehan, R.G. Beiko, A phylogenomic view of ecological specialization in the Lachnospiraceae, a family of digestive tract-associated bacteria, Genome Biol. Evol. 6 (2014) 703–713.
[41] H. Li, F. Liu, J. Lu, et al., Probiotic mixture of *Lactobacillus plantarum* strains improves lipid metabolism and gut microbiota structure in high fat diet-fed mice, Front. Microbiol. 11 (2020), 512.
[42] J. Li, T. Wu, N. Li, et al., Bilberry anthocyanin extract promotes intestinal barrier function and inhibits digestive enzyme activity by regulating the gut microbiota in aging rats, Food Funct. 10 (2019) 333–343.
[43] Y.-H. Chen, Z. Yu, L. Fu, et al., Vitamin D3 inhibits lipopolysaccharide-induced placental inflammation through reinforcing interaction between vitamin D receptor and nuclear factor kappa B p65 subunit, Sci. Rep. 5 (2015), 10871.
[44] L.-C. Tong, Y. Wang, Z.-B. Wang, et al., Propionate ameliorates dextran Sodium sulfate-induced colitis by improving intestinal barrier function and reducing inflammation and oxidative stress, Front. Pharmacol. 7 (2016), 253.
[45] L. Hu, L. Jin, D. Xia, et al., Nitrate ameliorates dextran sodium sulfate-induced colitis by regulating the homeostasis of the intestinal microbiota, Free Radic. Biol. Med. 152 (2020) 609–621.

[46] R. Curciarello, K.E. Canziani, I. Salto, et al., Probiotic lactobacilli isolated from kefir promote down-regulation of inflammatory *Lamina propria* T cells from patients with active IBD, Front. Pharmacol. 12 (2021), 658026.
[47] M.R. Chorawala, S. Chauhan, R. Patel, et al., Cell wall contents of probiotics (*Lactobacillus* species) protect against lipopolysaccharide (LPS)-induced murine colitis by limiting immuno-inflammation and oxidative stress, Probiotics Antimicrob. Proteins 13 (2021) 1005–1017.
[48] V. Neubauer, E. Humer, E. Mann, et al., Effects of clay mineral supplementation on particle-associated and epimural microbiota, and gene expression in the rumen of cows fed high-concentrate diet, Anaerobe 59 (2019) 38–48.
[49] X. Gao, S. Chang, S. Liu, et al., Correlations between α-linolenic acid-improved multitissue homeostasis and gut microbiota in mice fed a high-fat diet, mSystems 5 (2020), e00391-20.
[50] C. Yang, M. Wang, X. Tang, et al., Effect of dietary amylose/amylopectin ratio on intestinal health and cecal microbes' profiles of weaned pigs undergoing feed transition or challenged with *Escherichia coli* lipopolysaccharide, Front. Microbiol. 12 (2021), 693839.